Photobleaching of Bacteriorhodopsin Solubilized with Triton X-100

Takanori Sasaki,[1,2,*] Masashi Sonoyama,[1,3] Makoto Demura,[2] and Shigeki Mitaku[1,3]

[1] Department of Biotechnology, Tokyo University of Agriculture and Technology, 2-24-16 Nakacho, Koganei, Tokyo 184-8588, Japan

[2] Division of Biological Sciences, Graduate School of Science, Hokkaido University, Sapporo 060-0810, Japan

[3] Present address: Department of Applied Physics, Graduate School of Engineering, Nagoya University, Furo-cho, Chikusa-ku, Nagoya 464-8603, Japan

- Corresponding author:
- Takanori Sasaki
- Division of Biological Sciences,
- Graduate School of Science,
- Hokkaido University,
- Sapporo 060-0810, Japan
- Phone: +81-11-706-2773

  Fax: +81-11-706-2771
- Email: sasaki@sci.hokudai.ac.jp

Abbreviations: bR, bacteriorhodopsin; CD, circular dichroic; OG, octyl-β-glucoside; TX100, Triton X-100;

ABSTRACT

In the current studies, we examined the effects of hexagonal lattice formation with lipid membranes on the structural stability of native bacteriorhodopsin (bR). Denaturation kinetic measurements for bR solubilized with the mild nonionic detergent, Triton X-100 (TX100), were performed in the dark and under illumination by visible light. The solubilized bR was stable in the dark over a wide concentration range of TX100 (1 to 200 mM). In purple membranes, a bilobed band was observed in visible circular dichroic spectra due to interactions between neighboring chromophores. At all concentrations of TX100, this was replaced by a single positive band. Upon illumination with visible light, TX100-solubilized bR clearly showed photobleaching to bacterioopsin. These experimental results suggest that photobleaching is due to a lack of intermolecular interactions inside the purple membrane lattice. Extensive kinetic measurements further revealed that the rate constant of photobleaching is strongly dependent on the detergent concentration, although the activation energy for photobleaching does not significantly change with the TX100 concentration. The mechanism of photobleaching for the solubilized bR is discussed with respect to detergent micelle properties.

INTRODUCTION

Bacteriorhodopsin (bR) is an intrinsic membrane protein in the purple membrane of *Halobacterium salinarum* and functions as a light-driven proton pump (1). BR is composed of seven transmembrane helices and forms a two-dimensional crystalline structure (2). The three-dimensional structure of bR at the ground state has been determined at high resolution (3-8). Upon light absorption, bR undergoes a photochemical reaction called a photocycle. The photocycle involves photointermediates K, L, M, N and O whose absorption spectra give different maxima, indicating structural changes during the photocycle (9,10). Information about dynamic structural changes responsible for proton pumping has been obtained from the recent accumulation of diffraction images of the photointermediates (11-15).

Recent extensive studies on the structural stability of bR in the dark and under light illumination over a wide temperature range have revealed a quasi-stable high-temperature state above 60˚C (16). When kept in the dark, bR is stable against heat; however, in the high-temperature state, the two-dimensional crystalline structure of bR in the purple membrane begins to melt and its irradiation by visible light leads to irreversible photobleaching. These results imply that protein-protein interactions in the crystalline structure are responsible for structural stability in the photointermediate (i.e., functional) states of bR (16,17). Further analyses of photobleaching kinetics have indicated heterogeneity in the structural stability of bR in the purple membrane when illuminated by visible light (17). In addition, the temperature dependence of hydroxylamine reactivity has suggested that water accessibility in the internal region of the bR molecule is remarkably enhanced in an intermediate generated at high temperature (18).

Many studies have investigated the effects of solubilization on bR structures and photochemical reaction kinetics (19-28). These studies have shown that solubilized bR retains the proton-pumping activity although it has a photocycle different from native bR. It has been speculated that the difference in the photocycle is due to the loss of protein-protein interactions caused by monomerization and/or the loss of associated lipids. When solubilized with n-octyl-β-glucoside (OG), a mild detergent, bR undergoes an irreversible, single-component photobleaching upon continuous irradiation with visible light (29). It has been postulated that when bR is solubilized with OG, one or more photointermediates with low stability exist in the photocycle, due to loss of intermolecular interactions between protomers, leading to photobleaching mainly *via* the intermediate(s). However, because the OG-solubilized sample is unstable even in the dark, it is difficult to separately examine photobleaching and thermal bleaching in detail and to elucidate the main origin of photobleaching. Furthermore, it is significant to confirm whether the similar photobleaching phenomenon of the solubilized bR is observed with other kind of detergent or not.

In the present study, we compared the structural properties of native and detergent-solubilized bR and investigated the origin of photobleaching. For these studies, we examined the effect of another widely used mild non-ionic detergent, Triton X-100 (TX100), on the structural stability of bR in the dark and under visible light illumination. TX100 is a milder detergent than OG towards bR, and TX100-solubilized bR is relatively stable in the dark (19-20). Photoreaction kinetics have been examined for TX100-solubilized bR (19,20,24-28). Visible circular dichroism (CD) of purple membrane shows a band that is highly sesnsitive to the oligomerization state of protomers and is due to exciton coupling between neighboring

protomers; Upon solubilization of the purple membrane with TX100, the CD band with a bilobe profile is replaced with a broad positive band a broad positive band (30-32). In contrast, bR solubilized with OG exhibits no significant band (19).

Denaturation experiments at TX100 concentrations of 1 to 200 mM have shown that TX100-solubilized bR is highly stable in the dark up to approximately 50˚C, whereas even at 25˚C it is remarkably susceptible to irreversible photobleaching upon exposure to continuous irradiation with visible light. In the current studies, we found a significant increase in the rate constant of photobleaching with the increasing concentration of TX100 up to50 mM, above which the effect reached a plateau. The dependence of the rate constants of photobleaching on the concentration of TX100 is discussed in relation to changes in the size of TX100 micelles.

MATERIALS AND METHODS

Preparation of purple membrane suspension and TX100-solubilized bR

Purple membrane of *Halobacterium salinarum* strain R1M1 was prepared according to the method of Oesterhelt and Stoeckenius (34). The purified samples were suspended in 5 mM Tris-HCl (pH 7.0). The concentration of purple membrane was determined from the absorption maximum at 568 nm using an extinction coefficient of 62,700 $M^{-1}{\cdot}cm^{-1}$ (35). The concentration of purple membrane used for solubilization experiments was approximately 10 μM. Dark-adapted purple membrane was solubilized with 1 to 200 mM TX100 (Wako Pure Chemical Industries, Ltd., Osaka, Japan) in the dark for 2 h at 35˚C and then centrifuged at 105,000 × g for 60 min at 4˚C. The solubilized sample was obtained as the supernatant according to the method of Dencher and Heyn (19-20). The relative absorbances at the absorption maximum of

supernatants and precipitants treated with various concentrations of TX100 were observed to estimate the solubilization degree by comparing the absorbances of purple membrane prior to solubilization.

CD and absorption spectra measurements

CD spectra in the 300 to 750 nm region were recorded at 35˚C for the purple membrane and the TX100-solubilized bR using a J-820 spectropolarimeter (Jasco, Tokyo, Japan) with a thermostat-controlled cell holder. The speed and number of scans were 50 nm/min and 4 times, respectively. The path length of the optical cuvette was 10 mm. All CD measurements were performed in the dark. A DU7500 photodiode array spectrophotometer (Beckman Coulter, Fullerton, CA, USA) with a thermostat-controlled cell holder was used for measurements of absorption spectra of the solubilized bR and the purple membrane. Absorption spectra under constant illumination were obtained using a light illumination system that consisted of a xenon lamp source (average light power = 200 $mW \cdot cm^{-2}$), Y52 color filter, and heat-cut filter for filtering out the light wavelengths shorter than 520 nm and longer than 700 nm (36). Time-resolved absorption spectra under continuous illumination and in the dark were recorded at 3-min intervals for 60 min at 35˚C to 55˚C.

`RESULTS

1. Solubilization of purple membrane at low and high concentrations of the detergent TX100

Purple membrane prepared in this study showed an absorption maximum at 560 nm in the dark (Fig. 1A). There were marked increases in the turbidity around the ultraviolet region due to light scattering from membrane fragments. Purple membrane was solubilized with 1 to 6 mM TX100 and subjected to ultracentrifugation. The supernatants lacked the turbidity and showed a blue-shifted absorption band at 548 nm. This is in good agreement with previous reports (19, 37). No further changes in the absorption spectrum were observed when the concentration of TX100 was increased above 6 mM.

We further examined the solubilization degree of purple membrane as a function of TX100 concentration by determining the relative absorbance of the supernatant at λ_{max} compared to unsolubilized purple membrane (Fig. 1B). As shown in the inset of Fig. 1B, at the lower concentration region, the relative absorbance of the supernatant dramatically increased and reached a maximum of approximately 0.8. At concentrations of TX100 above 4 mM, there were no precipitates after centrifugation. These results suggest that the purple membrane was completely solubilized by concentrations of TX100 at or above 4 mM. When higher concentrations of TX100 were used for solubilization of the purple membrane, after a gradual decrease from the maximum of 0.8, the relative absorbance of the supernatant remained at a plateau of approximately 0.75. Similarly, bR completely solubilized with OG has been reported to show less absorbance than the original native sample (19).

Figure 2 shows the visible CD spectra of purple membrane and bR solubilized

with 5 mM TX100 or 50 mM OG. The CD spectrum of the purple membrane shows an asymmetric exciton band composed of two components: (a) a symmetric bilobed CD band due to exciton coupling between neighboring chromophores, and (b) a positive CD band that originates from interactions between apoprotein and chromophore (30-32). On the other hand, as previously reported (30-32), a broad single positive peak is observed for bR solubilized with TX100. Irrespective of the TX100 concentration used, the CD spectra were very similar (data not shown). The visible CD spectra for TX100- and OG-solubilized bR are remarkably different; the OG-solubilized sample shows a much flatter line (Fig. 2).

2. Effects of illumination on bleaching of bR solubilized with 5 mM TX100

The absorption spectra of bR solubilized with 5 mM TX100 were measured at 3-min intervals for 60 min in the dark and under illumination with visible light and across a temperature range of 35˚C to 55˚C. Representative spectra at 35˚C are shown in Fig. 3. In the dark at 35˚C, the solubilized bR showed no spectral changes during the measurement period, indicating that bR is highly stable in the dark even after solubilization with TX100. This is in striking contrast to the previous report that bR solubilized with OG shows gradual thermal bleaching at 35˚C even in the dark (29). Under illumination with visible light (Fig. 3B), however, TX100-solubilized bR clearly shows slow photobleaching. This photobleached protein did not recover the absorption band at 555 nm even a few hours after turning off the light. These results are similar to the previous findings with OG-solubilized bR (29).

The time course of the absorption decrease at λ_{max} in the dark and under illumination for bR solubilized with 5 mM TX100 at various temperatures are shown in

Figs. 4A and 4B, respectively. In the dark and at temperatures below 45˚C, the relative absorbance of the solubilized sample remains almost the same as the initial value during the measurement period, indicating that bR is highly stable to heat between 35˚C and 45˚C. At temperatures above 50˚C, however, decay of the relative absorbance is clearly observed, indicating a relatively slow thermal bleaching of the solubilized sample. And this thermal bleached sample did not recover even after cooling. Given that native bR undergoes thermal bleaching only at temperatures above 70˚C (16), it appears that, even in the dark, bR is destabilized by solubilization with TX100. On the other hand, under illumination with visible light, significant photobleaching is observed for the solubilized sample at 35˚C, and even at 25˚C, slow but significant photobleaching was observed for the solubilized bR (data not shown). These results show that photobleaching is remarkably accelerated at elevated temperatures.

We found that all of the decay curves obtained at 5 mM TX100 could be expressed as a single exponential decay function, which was used to determine the rate constants of bleaching. These rate constants were further analyzed with an Arrhenius plot to determine the activation energy for photobleaching of bR solubilized with 5 mM TX100 (Fig. 5). Except for the 55˚C point, the data (at temperatures of 35˚C to 55˚C) fitted to a straight line. The activation energy calculated from the slope was 16.9 kcal/mol. The activation energy for the photobleaching of the solubilized bR was similar to that reported for bR solubilized with 50 mM OG (12.5 kcal/mol) (29). It is likely that the deviation from a straight line at 55˚C in the Arrhenius plot is due to competition between thermal bleaching and photobleaching. We did not perform further analyses of rate constants of thermal bleaching in the dark because reliable kinetic data in this temperature range was limited.

3. Dependence of photobleaching of bR on the concentration of TX100

The effects of higher concentrations (5 to 200 mM) of TX100 on photobleaching kinetics were investigated at a constant temperature of 35˚C. All of the decay curves corresponded to a single exponential decay function (data not shown). Rate constants of photobleaching were calculated from these data with a curve-fitting procedure. Figure 6 shows the rate constants as a function of the TX100 concentration. The rate constants of photobleaching gradually increased as the concentration of TX100 was raised up to about 50 mM, after which they reached to a plateau of approximately 0.0013 s^{-1}. As in the case of sample solubilized with TX100 at concentrations below 5 mM, significant thermal bleaching was not observed in the dark at concentrations of TX100 above 5 mM (data not shown).

Further photobleaching kinetic measurements were carried out for bR solubilized with 10 to 50 mM TX100 and at temperatures of 35˚C to 55˚C. The Arrhenius plot for photobleaching of the solubilized samples under visible light illumination was obtained by fitting the absorbance changes at the absorption maximum to a single exponential decay function (Fig. 7). Irrespective of the detergent concentration, the activation energy for photobleaching calculated from the slopes was almost constant at approximately 19 kcal/mol. The frequency factor, on the other hand, became larger as the concentration of TX100 was increased.

DISCUSSION

Structure and thermostability of TX100-solubilized bR in the dark

The main purpose of the present study is to investigate effects of the hexagonal lattice of native bR in the purple membrane on its structure and stability in the dark and upon illumination with visible light. The structural properties and stability of TX100-solubilized bR can be discussed based on the experimental results obtained in this study in comparison with those of previous studies on bR in the purple membrane (16,17) and in OG-solubilized bR (29). Upon solubilization of the purple membrane with TX100, the CD spectrum in the visible region dramatically changed from a bilobe, which originates from interactions between neighboring chromophores, to a single positive band, and a blue shift of an absorption spectrum from 560 to 548 nm was observed. Based on this visible CD spectral change and other experimental results, it is thought that TX100-solubilized bR is in the monomeric state (19,38). Although experimental spectroscopic data for TX100-solubilized bR are limited because TX100 absorbs in the ultraviolet region, structural changes in bR molecules induced by monomerization can be discussed based on the spectral changes observed in this study. The most reasonable interpretations for the approximately 10-nm blue shift are a distribution shift of isomerization state of the chromophore toward a 13-*cis* configuration and/or changes of local structures around the Schiff base, such as the distance between D85 and the Schiff base (24, 26). The former can be excluded because the retinal isomer composition of the 13-*cis* and the all *trans* configuration in bR molecules has been reported to show no significant change upon solubilization with TX100 (39). Although a blue shift of 10 nm was observed in the absorption spectrum, the positive visible CD band, which is due to the local chiral structure around the

chromophore, and the high stability in the dark suggest that TX100 causes only relatively small structural changes in bR compared to the case of OG-solubilized bR. It is probable that TX100-solubilized bR retains a structure similar to native bR even after disruption of the hexagonal lattices. However, the onset temperature of thermal bleaching for the TX100-solubilized bR is approximately 20˚C lower than that observed for bR in native purple membrane, suggesting that protein-protein interaction in the two-dimensional crystals contributes significantly to stabilization of bR molecules in the dark.

It is well known that OG-solubilized bR is also in the monomeric state (21). A previous study on the denaturation of OG-solubilized bR indicated that it undergoes irreversible thermal bleaching in the dark even at 35˚C (29), whereas the present study showed that monomeric bR prepared by solubilization with TX100 is stable in the dark up to approximately 50˚C. Therefore, the structural stability of monomeric bR varies significantly depending on the detergent used for solubilization of the purple membrane. What structural properties are responsible for the difference in thermal stability between bR solubilized with TX100 and OG? Although it is possible that direct destabilization occurs due to interaction between detergent molecules and bR, in the current report, we focused on the structures of the protein in the detergent-protein complex. The absorption maximum of OG-solubilized bR showed a blue shift to 546 nm that was very similar to that in the TX100-solubilized sample. In addition, recent FT-Raman and FT-IR spectroscopic studies of OG-solubilized bR have revealed a significant shift in isomer composition of the retinal chromophore to a 13-*cis* enriched state coupled with conformational changes in the protein backbone (40). This is in a striking contrast to TX100-solubilized bR, which retains a structure around the chromophore similar to

native bR. These experimental results suggest that the preservation of the local environment around the retinal binding site is one of the key factors for stability of bR in the detergent-bR system in the dark.

As previously reported (19, 30-32), the CD spectrum in the visible region was very sensitive to oligomeric state of bR molecules. Based on the CD spectral change from an asymmetric spectrum to a single positive band (i.e., the disappearance of the exciton-coupled bilobe band due to a loss of interactions between neighboring chromophores), the present study showed that TX100-solubilized bR molecules are in a monomeric state. A similar positive CD band was also reported for purple membrane in the high-temperature state, and, even though bR molecules in this state are stable in the dark, they undergo irreversible photobleaching upon exposure to visible light (16-17). Similar to previous results by Decher et al. (19), when OG was used for solubilization, a flat CD signal (i.e., no significant CD signal) was observed. It is possible that the positive CD band, which originates from a chiral structure around the retinal chromophore, is a measure of stability of bR molecules in the dark.

Photobleaching of TX100-solubilized bR

This study clearly showed that TX100-solubilized bR, which is highly stable in the dark, undergoes remarkable photobleaching under continuous illumination with visible light. Even at 25˚C, photobleaching was observed for the solubilized bR (data not shown). It should be pointed out that the effects of photobleaching have not been considered in the previous studies on the structure and function of TX100-solubilized bR (19-20, 24-28). This is because the frequency of photobleaching in the photocycle of TX100-solubilized bR is only 3.94×10^{-3}% per cycle at 35˚C, based on the assumption

that the slowest photocycle of the TX-100 solubilized bR (life time) is approximately 160 ms (26). So that measurements must be made under light irradiation over a period of least 1 h to be able to detect photobleaching at room temperature by changes in the visible absorption.

It was previously reported that bR undergoes photobleaching in the OG-solubilized (29) and in the high-temperature intermediate states (16,17). As in the case of the TX100-solubilized bR, under these conditions, the two-dimensional crystalline structures are disrupted or considerably disordered. This photobleaching suggests the existence of a branching reaction of the photoreaction leading to bleaching. Although the molecular basis for the formation of the restoring force essential for the photocycle of native bR is not currently clear, protein-protein or protein-lipid interactions in the two-dimensional crystals must significantly contribute to the restoring force of active structures in the photocycle of bR.

An isosbestic point around 410 nm in the absorption spectra was clearly observed during photobleaching, and the decay of absorption at 555 nm fit to a single exponential function, similar to the photobleaching of the OG-solubilized bR (29). The activation energy for photobleaching of TX100-solubilized bR was only approximately 4 kcal/mol higher than for OG-solubilized bR even though, in the dark, TX100-solubilized bR was much more stable than OG-solubilized bR. Although the mechanism for bleaching by visible light remains unclear, these results suggest that bR solubilized with TX-100 or OG is bleached through a similar mechanism involving a branched reaction.

In contrast, for photobleaching of bR embedded in the purple membrane without detergents, double exponential curves were needed for kinetic analysis of experimental decay data. This suggests heterogeneity in the structural stability of bR in the purple

membrane to photobleaching (17). So it is plausible that the single-component photobleaching of the solubilized bR is due to a loss of heterogeneous protein-protein, or protein-lipid environment caused by complete disruption of the crystal structures in the purple membrane. Recently, a model has been proposed for the structural changes of bR in the purple membrane at high temperatures including possible pathways in the photocycle (18). In the proposed model, dynamic fluctuation of bR molecules due to the melting of the two-dimensional crystals are responsible for photobleaching, which occurs as a result of a lack or a weakening of the restoring force in the photocycle. This might also be true for photobleaching of the solubilized bR in the monomeric state.

As shown in Fig. 6, rate constants of photobleaching for the solubilized bR as a function of the detergent concentration indicated two phases: an increasing phase below 50 mM TX100 and a plateau phase between 50 to 200 mM TX100. For bR solubilized with TX100, a similar mechanism for photobleaching irrespective of concentrations of TX100 is suggested based on the fact that the activation energies for photobleaching changed very little. What is responsible for the increase in rate constants at concentrations below 50 mM? Although no detailed structural information of bR-detergent complexes is available, the properties of detergent micelles can provide some insight. Preliminary studies on the aggregation number of TX100 micelles using steady-state fluorescence quenching (32, 33) showed that the size of TX100 micelle becomes larger between 5 and 30 mM and reaches a plateau at higher concentrations (Sasaki et al., unpublished results). Additionally preliminary studies with ^{1}H-NMR spectroscopy have shown that the dynamics of TX100 micelle systems change significantly in the NMR time scale at TX100 concentrations below 50 mM (Sasaki et al., unpublished results). The physical properties determined by these two methods

showed a concentration dependence very similar to the rate constants of photobleaching. This suggests that, at concentrations of TX100 below 50 mM, acceleration of photobleaching is due to enhanced dynamic fluctuation of the bR-TX100 system with increasing TX100 micelle size.

Acknowledgements This work was supported by the Industrial Technology Research Grant Program of the New Energy and Industrial Technology Development Organization of Japan, and by grants-in-aid from the Ministry of Education, Culture, Science, Sports and Technology of Japan (Monbukagakusho).

REFERENCES

1. Bogomolni,R.A., R.A.Baker, R.H.Lozier and W.Stoekenius (1976) Light-driven proton translocations in *Halobacterium halobium*. *Biochim. Biophys. Acta*, **440**, 68-88.

2. Henderson,R. and P.N.T.Unwin (1975) Three-dimensional model of purple membrane obtained by electron microscopy. Nature, **257**, 28-32.

3. Luecke,H., B.Schobert, H.T.Richter, J.P.Cartailler and J.K.Lanyi (1999) Structure of bacteriorhodopsin at 1.55 Å resolution. *J. Mol. Biol*., **291**, 899-911.

4. Pebay-Peyroula,E., G.Rummel, J.P.Rosenbusch, and E.M.Landau (1997) X-ray structure of bacteriorhodopsin at 2.5 angstroms from microcrystals grown in lipidic cubic phases. *Science*, **277**, 1676-1681.

5. Kimura,Y., D.G.Vassylyev, A.Miyazawa, A.Kidera, M.Matsushima, K.Mitsuoka, K.Murata, T.Hirai and Y.Fujiyoshi (1997) Surface of bacteriorhodopsin revealed by high-resolution electron crystallography. *Nature*, **389**, 206-211.

6. Henderson,R., J.M.Baldwin, T.A.Ceska, F.Zemlin, E.Beckmann and K.H.Downing (1990) Model for the structure of bacteriorhodopsin based on high-resolution electron cryo-microscopy. *J. Mol. Biol*., **213**, 899-929.

7. Mitsuoka,K., T.Hirai, K.Murata, A.Miyazawa, A.Kidera, Y.Kimura and Y.Fujiyoshi (1999) The structure of bacteriorhodopsin at 3.0 Å resolution based on electron crystallography: implication of the charge distribution. *J. Mol. Biol*., **286**, 861-882.

8. Belrhali,H., P.Nollert, A.Royant, C.Menzel, J.P.Rosenbusch, E.M.Landau and E.Pebay-Peyroula (1999) Protein, lipid and water organization in bacteriorhodopsin crystals: a molecular view of the purple membrane at 1.9 Å resolution. *Structure Fold. Des*., **7**, 909-917.

9. Lozier,R.H., R.A.Bogomolni and W.Stoeckenius (1975)Bacteriorhodopsin: a light-driven proton pump in *Halobacterium Halobium*. *Biophys*. *J*., **15**, 955-962.

10. Lanyi,J.K. (1993) Proton translocation mechanism and energetics in the light-driven pump bacteriorhodopsin. *Biochim*. *Biophys*. *Acta*, **1183**, 241-261.

11. Edman,K., P.Nollert, A.Royant, H.Belrhali, E.Pebay-Peyroula, J.Hajdu, R.Neutze and E.M.Landau (1999) High-resolution X-ray structure of an early intermediate in the bacteriorhodopsin photocycle. *Nature*, **401**, 822-826.

12. Sass,H.J., G.Büldt, R.Gessenich, D.Hehn, D.Neff, R.Schlesinger, J.Berendzen and P.Ormos (2000) Structural alterations for proton translocation in the M state of wild-type bacteriorhodopsin. *Nature*, **406**, 649-653.

13. Luecke,H., B.Schobert, H.T.Richter, J.P.Cartailler and J.K.Lanyi (1999) Structural changes in bacteriorhodopsin during ion transport at 2 angstrom resolution. *Science*, **286**, 255-260.

14. Luecke,H., B.Schobert, J.P.Cartailler, H.T.Richter, A.Rosengarth, R.Needleman and J.K.Lanyi (2000) Coupling photoisomerization of retinal to directional transport in bacteriorhodopsin. *J.Mol.Biol*., **300**, 1237-1255.

15. Royant,A., K.Edman, T.Ursby, E.Pebay-Peyroula, E.M.Landau and R.Neutze (2000) Helix deformation is coupled to vectorial proton transport in the photocycle of bacteriorhodopsin. *Nature*, **406**, 645-648.

16. Yokoyama,Y., M.Sonoyama and S.Mitaku (2002) Irreversible photobleaching of bacteriorhodopsin in a high-temperature intermediate state. *J. Biochem*., **131**, 785-790.

17. Yokoyama,Y., M.Sonoyama and S.Mitaku (2004) Inhomogeneous stability of bacteriorhodopsin in purple membrane against photobleaching at high temperature.

Proteins, **54**, 442-54.

18. Sonoyama,M., and S.Mitaku (2004) High-temperature intermediate state of bacteriorhodopsin prior to the premelting transition of purple membrane revealed by reactivity with hydrolysis reagent hydroxylamine. *J. Phys. Chem. B*, **108**, 19496-19500.
19. Dencher,N.A. and M.P.Heyn (1978) Formation and properties of bacteriorhodopsin monomers in the non-ionic detergents octyl-β-D-glucoside and Triton X-100. *FEBS Lett*., **96**, 322-326.
20. Dencher,N.A. and M.P.Heyn (1982) Preparation and properties of monomeric bacteriorhodopsin. *Methods Enzymol*., **88**, 5-10.
21. Gottschalk,M., N.A.Dencher and B.Halle (2001) Microsecond exchange of internal water molecules in bacteriorhodopsin. *J. Mol. Biol*., **311**, 605-621.
22. Lam,E. and L.Packer (1983) Nonionic detergent effects on spectroscopic characteristics and the photocycle of bacteriorhodopsin in purple membranes. *Arch. Biochem. Biophys*., **221**, 557-564.
23. Lopez,F., S.Lobasso, M.Colella, A.Agostiano and A.Corcelli (1999) Light-dependent and biochemical properties of two defferent bands of bacteriorhodopsin isolated on phenyl-Sepharose CL-4B. *Photochem. Photobiol*., **69**, 599-604.
24. Wang,J.-P., S.Link, C.D.Heyes and M.A.El-Sayed (2002) Comparison of the dynamics of the primary events of bacteriorhodopsin in its trimeric and monomeric states. *Biophys. J*., **83**, 1557-1566.
25. Varo,G. and J.K.Lanyi (1991) Kinetic and spectroscopic evidence for an irreversible step between deprotonation and reprotonation of the Schiff base in the

bacteriorhodopsin photocycle. *Biochemistry*, **30**, 5008-5015.

26. Milder,S.J., T.E.Thorgeirsson, L.J.W.Miercke, R.M.Stroud and D.S.Kliger (1991) Effects of detergent environments on the photocycle of purified monomeric bacteriorhodopsin. *Biochemistry*, **30**, 1751-1761.

27. Hwang,S.B. and W.Stoeckenius (1977) Purple membrane vesicles: morphology and proton translocation. *J. Membr. Biol.*, **33**, 325-350.

28. Heyes,C.D. and M.A.El-Sayed (2003) Proton transfer reactions in native and deionized bacteriorhodopsin upon delipidation and monomerization. *Biophys. J.*, **85**, 426-434.

29. Mukai,Y., N.Kamo and S.Mitaku (1999) Light-induced denaturation of bacteriorhodopsin solubilized by octyl-β-glucoside. *Protein Eng.*, **12**, 755-759.

30. Heyn,M.P., P.-J.Bauer and N.A.Dencher (1975) A natural CD label to probe the structure of the purple membrane from *Halobacterium halobium* by means of exciton coupling effects. *Biochem. Biophys. Res. Commun.*, **67**, 897-903.

31. Bauer,P-J. and N.A.Dencher (1976) Evidence for chromophore-chromophore interactions in the purple membrane from reconstitution experiments of the chromophore-free membrane. *Biophys. Struct. Mechanism*, **2**, 79-92.

32. Isenbarger,T.A. and M.P.Krebs (2001) Thermodynamic stability of the bacteriorhodopsin lattice as measured by lipid dilution. *Biochemistry*, **40**, 11923-11931.

33. Turro,N.J. and A.Yekta (1978) Luminescent probes for detergent solutions. A simple procedure for determination of the mean aggregation number of micelles. *J. Am. Chem. Soc.* **100**, 5951-5952.

34. Oesterhelt,D. and W.Stoeckenius (1974) Isolation of the cell membrane of

Halobacterium halobium and its fractionation into red and purple membrane. *Methods Enzymol*., **31**, 667-678.

35. Rehorek,M. and M.P.Heyn (1979) Binding of all-trans-retinal to the purple membranes. Evidence for cooperativity and determination of the extinction coefficient. *Biochemistry*, **18**, 4977-4983.
36. Etoh,A., H.Itoh and S.Mitaku (1997) Light-induced denaturation of bacteriorhodopsin just above melting point of two-dimensional Crystal. J. *Phys*. *Soc*. *Jpn*., **66**, 975-978.
37. Meyer,O., M.Ollivon and M.T.Paternostre (1992) Solubilization steps of dark-adapted purple membrane by Triton X-100 A spectroscopic study. *FEBS Lett*., **305**, 249-253.
38. Reynolds,J.A. and W.Stoeckenius (1977) Molecular weight of bacteriorhodopsin solubilized in Triton X-100. *Proc*. *Natl*. *Acad*. *Sci*. *USA*., **74**, 2803-2804.
39. Scherrer,P., M.K.Mathew, W.Sperling and W.Stoeckenius (1989) Retinal isomer ratio in dark-adapted purple membrane and bacteriorhodopsin monomers. *Biochemistry*. **28**, 829-834.
40. Sonoyama,M., T.Hasegawa, T.Nakano and S.Mitaku (2004) Isomerization of retinal chromophore and conformational changes in membrane protein bacteriorhodopsin by solubilization with a mild non-ionic detergent, n-octyl- -glucoside: an FT-Raman and FT-IR spectroscopic study. *Vibrational Spectroscopy*, **35**, 115-119.

Figure captions

Figure 1 (A) Absorption spectra of bR solubilized with 1 to 6 mM TX100 (pH 7.0, 35˚C). Purple membrane was solubilized with TX-100, centrifuged, and spectra were obtained using the supernatant. (B) Relative absorbance of bR solubilized with 1 to 200 mM Triton X100 (pH 7.0, 35˚C). Inset: relative absorbance of bR solubilized with 1 to 6 mM TX100. Supernatant (●) and pellet (○) after the centrifugation.

Figure 2 Visible CD spectra of purple membrane and of bR solubilized with 5 mM TX100 or 50 mM OG (pH 7.0, 35˚C).

Figure 3 Absorption spectra in the dark (A) and under illumination with visible light (B) for bR solubilized with 5 mM TX100. Arrows indicate the changes in the absorption spectra (pH 7.0, 35˚C).

Figure 4 Absorption changes at λ_{max} in the dark (A) and under light illumination (B) observed at various temperatures for bR solubilized with 5 mM TX100. The absorption was measured over a 1-h period at 35˚C (●), 40˚C (■), 45˚C (○), 50˚C (▲), and 55˚C (◆) (pH 7.0).

Figure 5 Arrhenius plot of the bleaching rate for bR solubilized with 5 mM TX100 under illumination with visible light at 35˚C to 55˚C (pH 7.0).

Figure 6 TX100 concentration dependence of the bleaching rate for bR solubilized with

6 to 200 mM TX100 under illumination with visible light at 35˚C (pH 7.0).

Figure 7 Arrhenius plot of the bleaching rate of bR solubilized with 5 mM (●), 10 mM (▲), or 50 mM (◆) TX100 under illumination with visible light at 35˚C to 50˚C (pH 7.0).

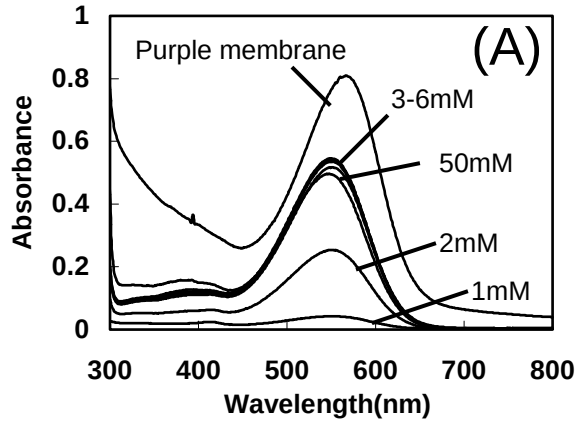

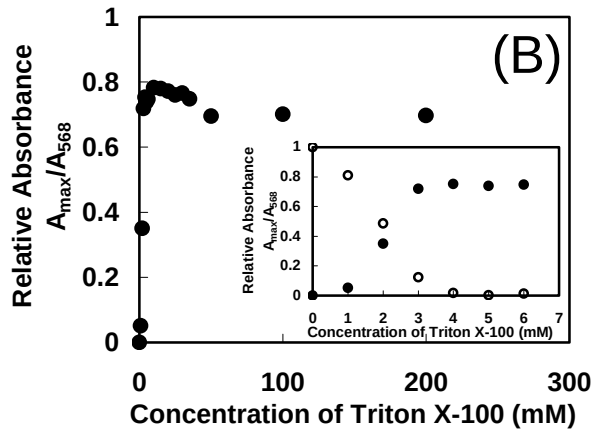

Figure 1 Sasaki et al.

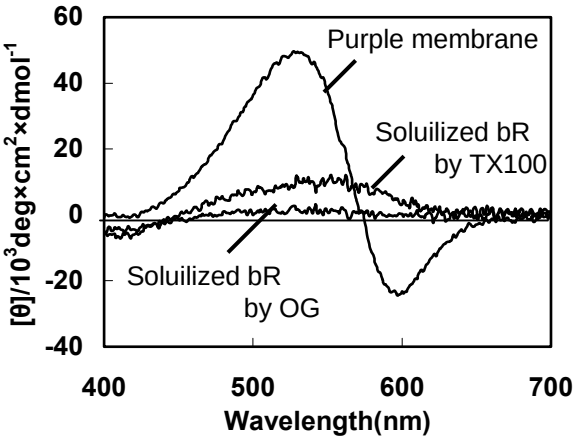

Figure 2 Sasaki et al.

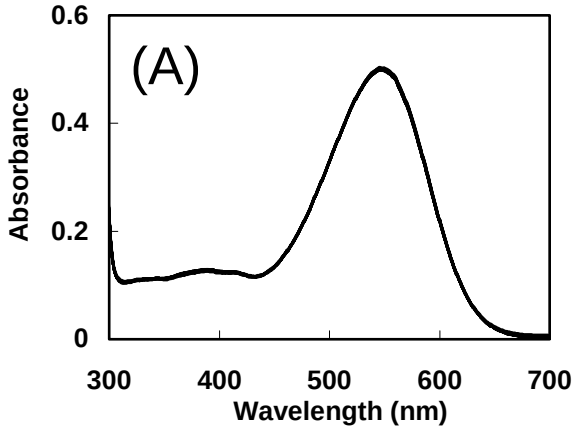

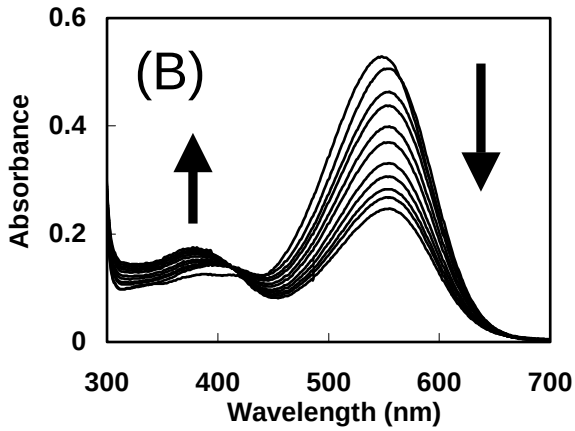

Figure 3 Sasaki et al.

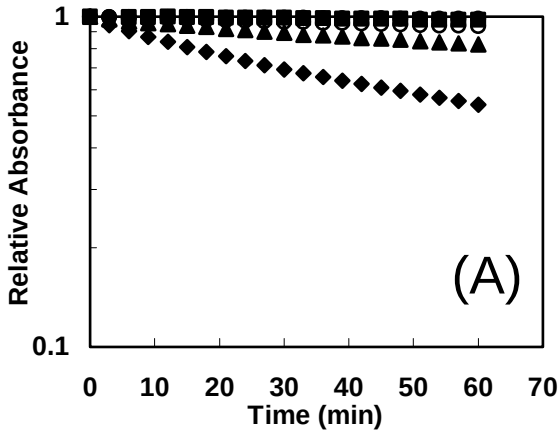

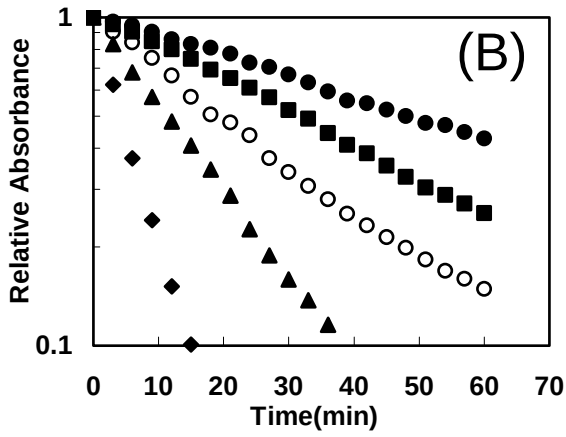

Figure 4 Sasaki et al.

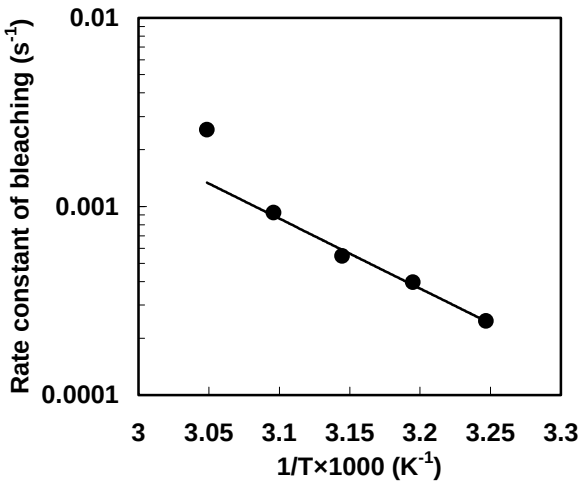

Figure 5 Sasaki et al.

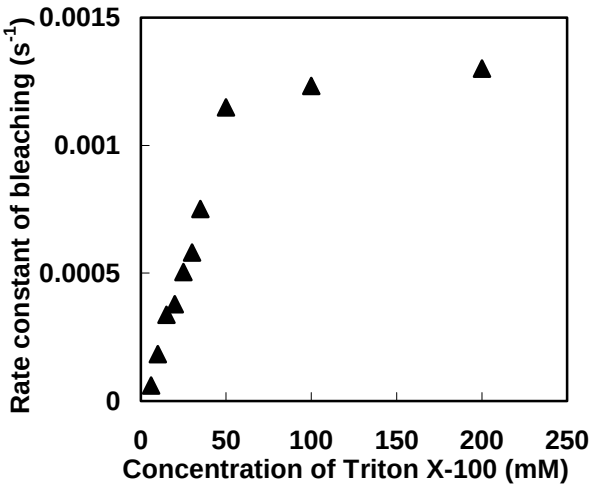

Figure 6 Sasaki et al.

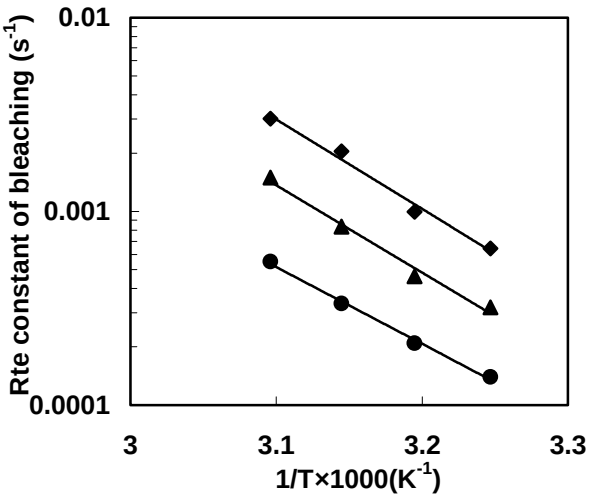

Figure 7 Sasaki et al